# Photoinduced Separation of Strongly Interacting 2-D Layered TiS2 Nanodiscs in Solution

**ARTICLE** *in* THE JOURNAL OF PHYSICAL CHEMISTRY C · MAY 2014

Impact Factor: 4.77 · DOI: 10.1021/jp5038624



**7 AUTHORS**, INCLUDING:

Daniel Rossi
Texas A&M University
**3** PUBLICATIONS **2** CITATIONS
SEE PROFILE

Jae Hyo Han
Yonsei University
**9** PUBLICATIONS **107** CITATIONS
SEE PROFILE

THE JOURNAL OF PHYSICAL CHEMISTRY C

Article

pubs.acs.org/JPCC

# Photoinduced Separation of Strongly Interacting 2-D Layered $TiS_2$ Nanodiscs in Solution

Daniel Rossi,[†] Jae Hyo Han,[‡] Dongwon Yoo,[‡] Yitong Dong,[†] Yerok Park,[†] Jinwoo Cheon,*[,‡] and Dong Hee Son*[,†]

[†]Department of Chemistry, Texas A&M University, College Station, Texas 77845, United States

[‡]Department of Chemistry,Yonsei University, Seoul 120-749, Korea

Supporting Information

**ABSTRACT:** Colloidal 2-D layered transition metal dichalcogenide (TMDC) nanodiscs synthesized with uniform diameter and thickness can readily form the vertically stacked assemblies of particles in solution due to strong interparticle cohesive energy. The interparticle electronic coupling that modifies their optical and electronic properties poses a significant challenge in exploring their unique properties influenced by the anisotropic quantum confinement in different directions taking advantage of the controlled diameter and thickness. Here, we show that the assemblies of 2-D layered $TiS_2$ nanodiscs are efficiently separated into individual nanodiscs via photoexcitation of the charge carriers by pulsed laser light, enabling the characterization of the properties of noninteracting $TiS_2$ nanodiscs. Photoinduced separation of the nanodiscs is considered to occur via transient weakening of the interparticle cohesive force by the dense photoexcited charge carriers, which facilitates the solvation of each nanodisc by the solvent molecules.

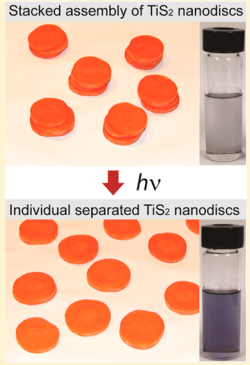


## INTRODUCTION

Atomically thin 2-D layered transition metal dichalcogenide (TMDC) nanostructures are attracting much attention due to their material properties that are sensitive to the number of layers and the strength of their interlayer interaction.[1−4] Often these materials are synthesized via exfoliation from bulk or using chemical vapor deposition (CVD) methods, which produce single and few-layer thin flakes enabling detailed studies of the thickness-dependent material properties of TMDC.[1,5−7] Recently, solution-phase synthesis methods have been developed for several TMDC materials, enabling the production of uniform ensembles of colloidal TMDC nanodiscs with simultaneously controlled thickness and lateral area.[8] Colloidal 2-D layered TMDC nanodiscs with controllable thickness and area provide a unique opportunity to explore the material properties correlated with both variation of interlayer interaction and intralayer spatial confinement that are expected to be highly anisotropic.[1]

Optical absorption has frequently been used to correlate the electronic structure with the dimensions or morphology of the colloidal nanoparticles, provided that the size and shape distributions are narrow and that the particles are well separated within the solution.[9,10] In typical colloidal solutions of inorganic nanoparticles, surface-bound ligands or surface ions provide the colloidal stability, keeping the particles separated from each other. Ordered assemblies or aggregates of the interacting particles can also form within the solution depending on the factors that determine the balance between interparticle cohesive energy and particle solvation, such as surface passivation, solvent polarity, etc. Interparticle interactions and the formation of the assemblies of interacting particles is an important issue since the electronic, optical, and transport properties of the particles can change significantly via electronic coupling.[11−15] Colloidal 2-D layered TMDC nanodiscs have large flat basal planes, and the possible interparticle contact area that affects interparticle cohesive energy and electronic coupling is much larger than that in 0-D and 1-D structures of the same volume. Therefore, the formation of an interacting assembly of particles is more facile than that in 0-D and 1-D structures, and its effect on the optical and electronic properties can also be more significant.[16,17] The alteration of the optical properties due to interparticle electronic coupling can pose a challenge in exploring the unique dimensionally anisotropic properties of transition metal dichalcogenide nanostructures using colloidal nanoparticles with well-controlled lateral and transverse dimensions.

In this study, we show that the vertically stacked assemblies of $TiS_2$ nanodiscs present in the colloidal solution due to the strong interparticle interaction via basal planes can be readily separated into individual noninteracting nanodiscs via pulsed photoexcitation. Interband photoexcitation of $TiS_2$ nanodiscs with pulsed laser light creates dense charge carriers that transiently modify the charge distribution within the nanodiscs. The change in charge distribution in $TiS_2$ nanodiscs during the lifetime of the charge carriers is considered to nonthermally weaken the interparticle cohesive energy and facilitate the

**Received:** April 20, 2014
**Revised:** May 16, 2014
**Published:** May 16, 2014





dx.doi.org/10.1021/jp5038624 | J. Phys. Chem. C 2014, 118, 12568−12573

solvation of each nanodisc by the solvent molecules as illustrated in Figure 1. Since the basal planes of $TiS_2$ are

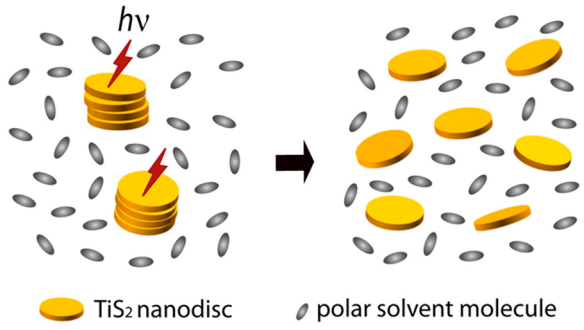


**Figure 1.** Separation of strongly interacting colloidal 2-D layered $TiS_2$ nanodiscs via photoinduced weakening of interparticle cohesive energy that facilitates the solvation of each nanodisc.

polar, photoinduced separation was particularly efficient in polar solvent media. The capability to optically modify the interparticle interaction and prepare noninteracting colloidal TMDC nanoparticles in solution will be important in exploring their properties correlated with lateral and transverse dimensions without contamination from the strong interparticle coupling.

## EXPERIMENTAL SECTION

**Material Preparation and Characterization.** We chose $TiS_2$ in this study taking advantage of the relatively well-established control of the diameter and thickness as reported in recent work by Cheon et al.[18] $TiS_2$ nanodiscs passivated with oleylamine were synthesized following the procedures reported therein. In this study, two $TiS_2$ nanodisc samples of different average diameter ($d$) and thickness ($t$) passivated with oleylamine were prepared. One has $d$ = 53 nm ($\sigma$ = 10 nm) and $t$ = 7 nm ($\sigma$ = 1.1 nm), and the other has $d$ = 150 nm ($\sigma$ = 25 nm) and $t$ = 9.5 nm ($\sigma$ = 1.7 nm), where $\sigma$ is the standard deviation. Each sample is referred to as $d$ = 50 nm and $d$ = 150 nm nanodiscs, respectively, hereafter. Briefly, $TiS_2$ nanodiscs were synthesized by adding $CS_2$ to the mixture of $TiCl_4$ and oleylamine at 300 °C. The size of the nanodiscs were controlled by adjusting the concentration of the precursors. X-ray diffraction (XRD) patterns of $TiS_2$ nanodiscs were obtained on a Bruker-AXS D8 powder diffractometer with a Cu-$\alpha$ X-ray source. Transmission electron micrographs (TEMs) were obtained with FEI Tecnai G2 F20 FE-TEM operating at 200 kV. The molar extinction coefficient of $TiS_2$ nanodiscs used to estimate the photoexcitation density was obtained from the particle size measured from TEM and concentration of Ti ions from the elemental analysis. The elemental analysis was performed employing inductively coupled plasma mass spectrometry (PerkinElmer DRCII ICP-MS) using commercial ICP standard solution for Ti ions (Fluka). For $d$ = 150 nm $TiS_2$ nanodiscs, the extinction coefficient at the photoexcitation wavelength of 800 nm was determined to be ~3.4 × $10^9$ $M^{-1}cm^{-1}$.

**Photoinduced Separation of Nanodiscs.** Photoinduced separation of the assembly of $TiS_2$ nanodiscs was studied using *cw* and pulsed laser light at 800 nm produced from a Ti:sapphire oscillator and amplifier (KMLabs), respectively, which are resonant with a higher-energy interband transition in $TiS_2$ above the band gap. The colloidal $TiS_2$ nanodisc solution (3 mL) dispersed in thoroughly deoxygenated solvent was constantly stirred during the photoexcitation in a quartz cuvette. The average intensities of both *cw* and pulsed laser light at 800 nm were kept at 1.4 W/$cm^2$. The pulse width and the repetition rate of the pulsed laser light were ~100 fs and 3 kHz, respectively. A 405 nm *cw* diode laser (CrystaLaser) was also used to examine the wavelength dependence of the photoinduced separation of $TiS_2$ nanodiscs. The extinction spectra of $TiS_2$ nanodisc solutions were taken with a Hitachi U-4100 UV/vis/NIR spectrophotometer or a CCD-based UV−vis spectrometer from Ocean optics (USB4000). Dynamic light scattering (DLS) from the colloidal $TiS_2$ nanodisc solution was measured to examine the change in the effective hydrodynamic diameter of the particles due to photoexcitation and ultrasonication. For this purpose, a DLS system (Brookhaven Instruments Co.) equipped with a digital autocorrelator was used in conjunction with an Ar ion laser (514.5 nm) as the light source. Since the distribution of the hydrodynamic diameter was estimated using the model assuming the spherical shape of particles, the values of the hydrodynamic diameter do not accurately represent the diameter or thickness of the $TiS_2$ nanodisc and should be interpreted on qualitative bases.

## RESULTS AND DISCUSSION

The photoinduced separation of the assemblies of the strongly interacting $TiS_2$ nanodiscs and the consequent changes in the optical properties were studied from the measurements of the optical extinction spectra and dynamic light scattering (DLS) and X-ray diffraction patterns. Transmission electron micrographs of the colloidal $TiS_2$ nanodiscs before and after the photoexcitation were obtained to examine the morphology of the assemblies and individual nanodiscs. The effects of ultrasonication, commonly used to disperse the interacting nanoparticles, on the optical extinction and DLS are also contrasted with those of the photoexcitation.

Figure 2a,b shows the effects of photoexcitation and ultrasonication on the optical extinction spectra of colloidal $TiS_2$ nanodiscs of two different sizes ($d$ = 50 and 150 nm) dispersed in deoxygenated chloroform. Blue and green curves are the spectra of the as-synthesized $TiS_2$ samples with 1 and 10 h of ultrasonication, respectively. Red curves are from the samples after 1 h of ultrasonication and an additional 10 min of pulsed photoexcitation at 800 nm (1.4 W/$cm^2$, ~100 fs, 3 kHz repetition rate). The broad peaks in the visible and near-infrared region are attributed to the higher-energy interband transitions above the bulk bandgap of roughly 0.1 eV.[5,19,20] Both nanodisc samples exhibit qualitatively similar spectral features. However, the peaks occur at the shorter wavelengths in the smaller nanodiscs, which may reflect the confinement in lateral or (and) transverse dimensions. Figure 2c,d is the effective hydrodynamic diameter distributions corresponding to Figure 2a,b, estimated from the DLS measurements. With increasing ultrasonication time and with photoexcitation, the distribution of hydrodynamic diameter shifts to the smaller values. In this study, we will interpret DLS data rather qualitatively since the data was analyzed with a model assuming the spherical particle shape that is limited in describing the behavior of the disc-shaped particles.

An important feature observed in Figure 2a−d is that the optical extinction spectra of the colloidal $TiS_2$ nanodiscs vary with the size of the assembly of the interacting nanodiscs. In the $d$ = 150 nm sample, the peak near 600 nm, assigned to the interband transition from right below the Fermi level to the


dx.doi.org/10.1021/jp5038624 | J. Phys. Chem. C 2014, 118, 12568−12573

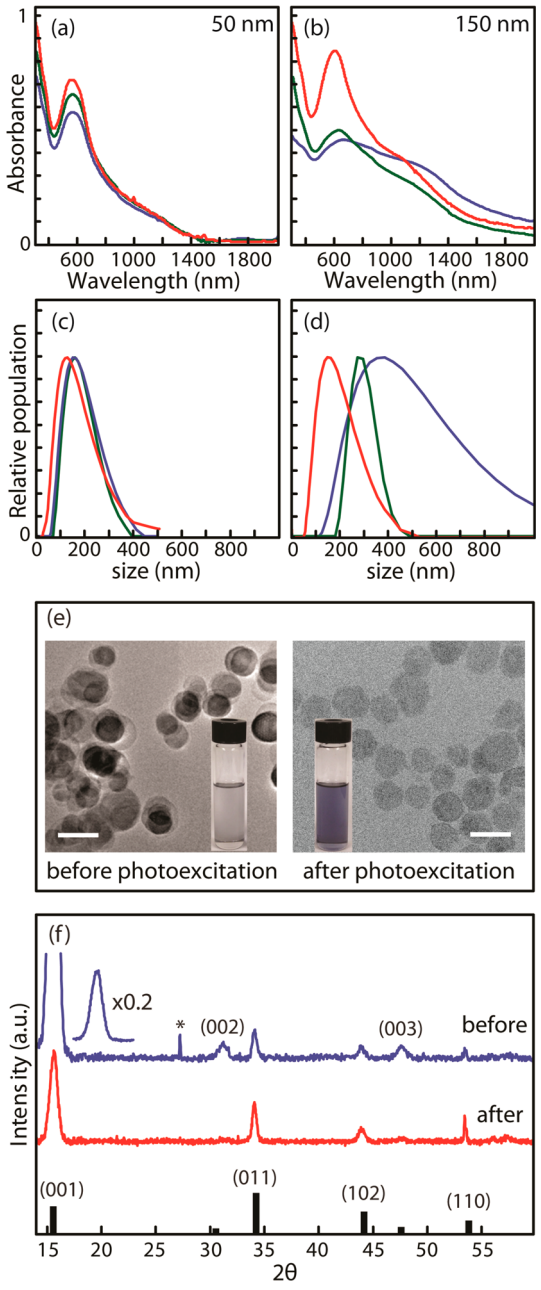


**Figure 2.** (a,b) Extinction spectra and (c,d) effective hydrodynamic diameter distributions of the colloidal $TiS_2$ nanodiscs of two different sizes after ultrasonication or photoexcitation. Blue, 1 h ultrasonication; green, 10 h ultrasonication; and red, 1 h ultrasonication and 10 min of pulsed photoexcitation at 800 nm. $d$ = 50 nm for a and c, and $d$ = 150 nm for b and d. (e) TEM image of the $d$ = 150 nm $TiS_2$ sample before and after 30 min of photoexcitation. The scale bar is 200 nm. (f) XRD patterns of $d$ = 150 nm $TiS_2$ nanodiscs before and after 30 min of photoexcitation. The vertical bars represent the standard XRD pattern of bulk $TiS_2$ (ICSD #: 000-015-0853). * is noise.

band in Σ M direction,[20] blueshifts with a significant increase in the intensity as the hydrodynamic diameter decreases. The blueshift in the extinction spectra with decreasing size of the nanodiscs assembly may be interpreted as the decreasing extent of the interparticle electronic coupling that widens the gap between the bands.[7,21] In the $d$ = 50 nm sample, spectral change in the extinction spectra by ultrasonication and photoexcitation is less pronounced than that in the $d$ = 150 nm sample, while the trend is similar. The relatively weak effect of the photoexcitation and ultrasonication in $d$ = 50 nm nanodiscs is likely due to the smaller interparticle cohesive energy resulting in the lower extent of assembly formation than that in the nanodiscs with the larger diameter. The tendency to form the assemblies of the interacting particles in the chemically synthesized $TiS_2$ nanodiscs can be understood from the relatively poor passivation of the flat basal planes during synthesis. In 2-D layered TMDC nanodiscs, the basal planes are composed of chalcogens with no dangling bonds, whereas the atoms at the edges are not fully coordinated. Therefore, oleylamine used as the surfactant will bind preferentially to the edge atoms during the synthesis and leave the basal planes exposed for more facile interparticle interaction and the formation of vertically stacked assemblies along the $c$-axis as shown in Figure 2e.[22,23]

Another noteworthy observation in Figure 2 is that the photoexcitation is much more efficient in separating the assemblies of $d$ = 150 nm $TiS_2$ nanodiscs than ultrasonication. In fact, nearly complete separation of the assemblies into individual $TiS_2$ nanodiscs could be achieved after tens of minutes of photoexcitation as will be discussed later, whereas ultrasonication can only reduce the size of the assemblies even after 10 h. TEM images in Figure 2e show that the vertically stacked assemblies of $TiS_2$ nanodiscs present in the sample before the photoexcitation are well separated after 30 min of photoexcitation. The resulting changes in the optical extinction spectra are clearly visible in the photographs of the sample before and after the photoexcitation shown in Figure 2e. XRD patterns in Figure 2f also indicate that the lattice structure of $TiS_2$ nanodiscs remains the same after the photoexcitation. However, (001), (002), and (003) diffraction peaks attenuated significantly after the photoexcitation, consistent with the removal of the stacking along the $c$-axis. No sign of photoinduced structural degradation or change in diameter and thickness of the nanodiscs was observed in TEM images, when the deoxygenated solvents were used to prevent photooxidation (Figure S1 in Supporting Information). The average thickness of $d$ = 150 nm $TiS_2$ nanodiscs after photoexcitation was $t$ = 9.0 nm ($\sigma$ = 1.5 nm), which is nearly identical to that of the sample before photoexcitation. However, partial photooxidation of $TiS_2$ to $TiO_2$ can occur in the presence of the dissolved oxygen in solvent and the resulting $TiS_2/TiO_2$ heterostructures are readily identified in TEM and XRD as shown in Figure S3 of Supporting Information.[24,25]

The data in Figure 2 indicate that photoexcitation can separate the strongly interacting $TiS_2$ nanodiscs, which may be more generally applicable in other layered colloidal transition metal dichalcogenide nanodiscs if the same mechanism is in operation. In order to gain insight into the mechanism of the photoinduced separation of the strongly interacting $TiS_2$ nanodiscs, several comparative analyses were made under varying photoexcitation conditions and in solvents with different polarities. Figure 3a,c shows the effect of *cw* and pulsed photoexcitation on the extinction spectrum of $d$ = 150 nm $TiS_2$ nanodiscs dispersed in deoxygenated chloroform as a function of photoexcitation time. Both *cw* and pulsed laser beams at 800 nm had the same average intensity of ~1.4 W/cm$^2$. The variations of the peak position and intensity are plotted in Figure 3b,d. A blueshift and an increase in intensity of the interband absorption peak were observed only with the pulsed excitation, whereas *cw* excitation had no effect. Furthermore, the spectral blueshift and increase of the intensity


dx.doi.org/10.1021/jp5038624 | J. Phys. Chem. C 2014, 118, 12568−12573

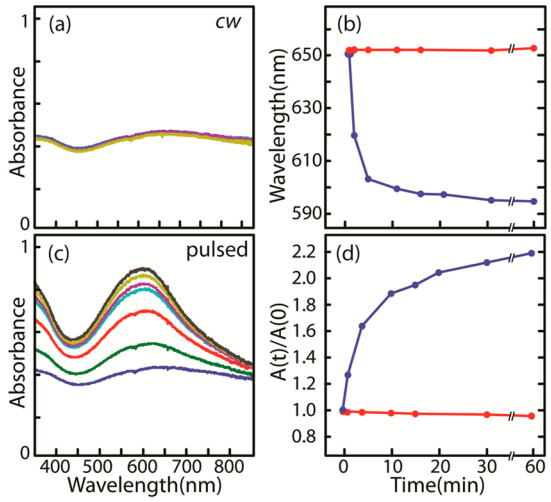


**Figure 3.** (a,c) The time-variation of the absorption spectra of $d$ = 150 nm $TiS_2$ nanodiscs in chloroform under (a) *cw* and (c) pulsed laser irradiation conditions. (b) Time dependence of the peak position under *cw* (red) and pulsed (blue) laser irradiation. (d) Time dependence of the peak intensity, A(t), normalized to the initial intensity, A(0), under *cw* (red) and pulsed (blue) laser irradiation.

saturated in ~10 and ~30 min, respectively, with negligible additional change up to 120 min of continued photoexcitation. Considering that the TEM image of the $TiS_2$ nanodiscs after 30 min with pulsed photoexcitation shown in Figure 2e has mostly the isolated nanodiscs, the saturation of the blueshift and intensity of the peak can be interpreted as the completion of the separation of the interacting nanodiscs.

While it is intriguing that only the pulsed excitation is capable of dispersing the assembly of interacting $TiS_2$ nanodiscs and induces a large spectral change, it provides useful insight into the possible mechanisms of photoinduced separation. We ruled out direct heating of the lattice by the absorbed photons as the possible cause of the photoinduced separation of the nanodiscs. The upper limit of the local lattice heating in each nanodisc, assuming no heat dissipation to the solvent, was only $\Delta T$ = 20 °C under the pulsed excitation condition based on the extinction coefficient of the nanodisc and the fluence of the excitation light (see Supporting Information). Actual local lattice heating should be significantly lower than this estimate due to the rapid heat dissipation from the lattice to the solvent. Steady-state heating of the entire colloidal solution at 40 °C (20 °C higher than the ambient temperature) had no effect on the optical spectra and dispersion of $TiS_2$ nanodiscs, ruling out the local lattice heating as the driving force for the photoinduced separation. We also ruled out the potential involvement of the two-photon process since *cw* excitation at 405 nm with comparable intensity did not have any effect on the extinction spectrum.

Photoinduced separation of the interacting nanodiscs only by the pulsed excitation may be explained by the relatively high *instantaneous* excitation density ($2.4 \times 10^4$/particle in $d$ = 150 $TiS_2$; see Supporting Information) from each pulsed excitation in contrast to the low *steady-state* excitation density ($7.3 \times 10^{-2}$/ns·particle in $d$ = 150 nm $TiS_2$) from *cw* excitation. The interband excitation shifts charge distribution from S to Ti, and potential trapping of the charge carriers will accumulate localized charges at the trapping site, such as the surface of the nanodiscs, during their lifetime of a few to tens of nanoseconds.[26] Therefore, the pulsed excitation will transiently modify the charge distribution in $TiS_2$ nanodiscs, whose magnitude increases with the *instantaneous* excitation density. If the transient modification of charge distribution is sufficiently large and capable of weakening the interparticle cohesive force, each laser pulse can provide an additional driving force favoring the solvation of the individual nanodiscs by the surrounding solvent molecules. Since the typical organic solvent molecules with a diffusion coefficient of $\sim 10^{-9}$ $m^2/s$ can self-diffuse ~10 nm in tens of nanoseconds, solvent molecules will have sufficient time to intervene between the nanodiscs taking advantage of the weakened cohesive force. The above hypothesis is also corroborated by the slower rate of spectral change observed from the photoexcitation with longer laser pulses (0.1−1 ns) of the same average intensity that produces the lower instantaneous excitation density due to the charge carrier relaxation during the period of pulse width.

To further test the hypothesis of the photoinduced separation via the facilitated solvation of $TiS_2$ nanodiscs, we compared the efficiency of the photoinduced separation of the nanodisc assemblies in solvents of varying polarities. Figure 4

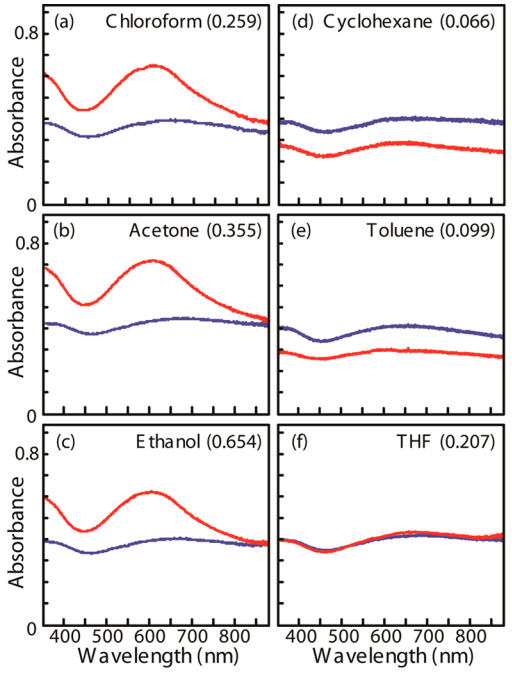


**Figure 4.** Effect of solvent polarity on laser-induced changes in the absorption spectra of $d$ = 150 nm $TiS_2$ nanodiscs. Blue and red curves are before and after 5 min of pulsed laser irradiation, respectively. The relative solvent polarity with respect to water is indicated in each panel.

compares the optical extinction spectra of $d$ = 150 nm $TiS_2$ nanodiscs before and after the pulsed photoexcitation for 5 min in each solvent. Interestingly, the spectral change was observed only in relatively polar solvents. In nonpolar solvents, such as cyclohexane and toluene, no spectral shift was observed even when the sample was photoexcited much longer. The decrease of the intensity after the photoexcitation in cyclohexane and toluene is due to the deposition of $TiS_2$ nanodiscs on the surface of the cuvette, not the degradation of the nanodiscs. The above observation indicates that photoinduced solvation of each $TiS_2$ nanodisc is preferred by the polar solvents, which is consistent with the polar nature of the exposed basal planes composed of S atoms. Unfavorable solvation of the polar


dx.doi.org/10.1021/jp5038624 | J. Phys. Chem. C 2014, 118, 12568−12573

surface with nonpolar solvents will explain the inability of cyclohexane and toluene to separate the interacting particles. The photoexcited $TiS_2$ nanodisc solutions in polar solvents retains the extinction spectra of the separated nanodiscs over a week. However, reformation of the interacting assembly can also be induced by changing the solvent polarity. Figure 5

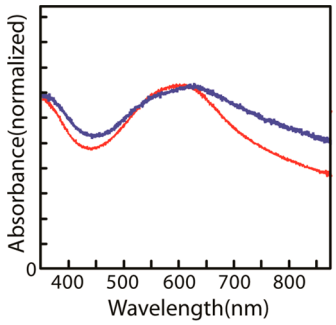


**Figure 5.** Reformation of the assembly of interacting $d$ = 150 nm $TiS_2$ nanodiscs by changing the solvent polarity. Red: photoexcited sample in deoxygenated chloroform. Blue: 20 h after the resuspension of the photoexcited $TiS_2$ nanodiscs in cyclohexane. The spectra are normalized to the peak intensities.

compares the extinction spectrum of the photoexcited $TiS_2$ nanodisc in deoxygenated chloroform with that obtained 20 h after replacing the solvent with cyclohexane by precipitation and resuspention of the nanodiscs. After the resuspension of the photoexcited $TiS_2$ nanodiscs in cyclohexane, the peak in the extinction spectra shifted to the longer wavelength indicating the formation of the assembled structure.

## CONCLUSIONS

In summary, we showed that the optical absorption of colloidal solutions of 2-D layered $TiS_2$ nanodiscs of controlled diameter and thickness is strongly affected by the assemblies of strongly interacting nanodiscs present within the solution. This poses a significant challenge in studying the electronic structure of the layered transition metal dichalcogenide nanoparticles correlated with the lateral and transverse dimensions. However, efficient separation of the strongly interacting nanodiscs into non-interacting particles can be achieved by using pulsed photo-excitation in polar solvents. Pulsed photoexcitation is considered to weaken the interparticle cohesive force and facilitate the solvation of individual particles by the solvent molecules via transient modification of the charge distribution in the nanodiscs. The ability to optically modify the interparticle interaction will be useful not only for the reliable optical characterization of the colloidal layered transition metal dichalcogenide nanoparticles but also for controlling the assembly of the interacting TMDC nanoparticles with light.

## ASSOCIATED CONTENT

### Supporting Information

TEM images from $d$ = 150 nm $TiS_2$ nanodiscs before and after laser exposure, TEM and PXRD of photooxidized $d$ = 150 nm $TiS_2$ nanodiscs, UV/vis extinction spectra from nanodisc solutions heated in a water bath showing that deaggregation is nonthermal, calculation of the molar extinction coefficient of $TiS_2$, and transient lattice temperature of the photoexcited $TiS_2$ nanodiscs. This material is available free of charge via the Internet at http://pubs.acs.org.

## AUTHOR INFORMATION

### Corresponding Authors

*(J.C.) Tel: 82-2-364-7050. E-mail: jcheon@yonsei.ac.kr.
*(D.H.S.) Tel: 979-458-2990. E-mail: dhson@chem.tamu.edu.

### Notes

The authors declare no competing financial interest.

## ACKNOWLEDGMENTS

This work was supported by NSF (DMR-0845645), Welch Foundation (A-1639) (to D.H.S), and the Creative Research Initiative (grant number 2010-0018286), Air Force Office of Scientific Research (BAA-AFOSR-2013-0001-BRI-1) (to J.C.). We also thank Gyo Seong Heo for assistance with DLS measurements.

## REFERENCES

(1) Chhowalla, M.; Shin, H. S.; Eda, G.; Li, L.; Loh, K. P.; Zhang, H. The Chemistry of Two-Dimensional Layered Transition Metal Dichalcogenide Nanosheets. *Nat. Chem.* **2013**, *5*, 263−375.
(2) Wang, Q. H.; Kalantar-Zadeh, K.; Kis, A.; Coleman, J. N.; Strano, M. S. Electronics and Optoelectronics of Two-Dimensional Transition Metal Dichalcogenides. *Nat. Nanotechnol.* **2012**, *7*, 699−712.
(3) Mak, K. F.; Lee, C.; Hone, J.; Shan, J.; Heinz, T. F. Atomically Thin $MoS_2$: A New Direct-Gap Semiconductor. *Phys. Rev. Lett.* **2010**, *5106*, 136805−136809.
(4) Butler, S. Z.; Hollen, S. M.; Cao, L.; Cui, Y.; Gupta, J. A.; Gutiarrez, H. R.; Heinz, T. F.; Hong, S. S.; Huang, J.; Ismach, A. F.; et al. Progress, Challenges, and Opportunities in Two-Dimensional Materials Beyond Graphene. *ACS Nano* **2013**, *7*, 2898−2926.
(5) Cheon, J.; Gozum, J. E.; Girolami, G. S. Chemical Vapor Deposition of $MoS_2$ and $TiS_2$ Films From the Metal−Organic Precursors $Mo(S\text{-}t\text{-}Bu)_4$ and $Ti(S\text{-}t\text{-}Bu)_4$. *Chem. Mater.* **1997**, *9*, 1847−1858.
(6) Zhan, Y.; Liu, Z.; Najmaei, S.; Ajayan, P. M.; Lou, J. Large-Area Vapor-Phase Growth and Characterization of $MoS_2$ Atomic Layers on a $SiO_2$ Substrate. *Small* **2012**, *8*, 966−971.
(7) Eda, G.; Yamaguchi, H.; Voiry, D.; Fujita, T.; Chen, M.; Chhowalla, M. Photoluminescence from Chemically Exfoliated $MoS_2$. *Nano Lett.* **2011**, *11*, 5111−5116.
(8) Han, J. H.; Lee, S.; Cheon, J. Synthesis and Structural Transformations of Colloidal 2D Layered Metal Chalcogenide Nanocrystals. *Chem. Soc. Rev.* **2013**, *42*, 2581−2591.
(9) Murray, C. B.; Norris, D. J.; Bawendi, M. G. Synthesis and Characterization of Nearly Monodisperse CdE (E=S, Se, Te) Semiconductor Nanocrystallites. *J. Am. Chem. Soc.* **1993**, *115*, 8706−8715.
(10) Burda, C.; Chen, X.; Narayanan, R.; El-Sayed, M. A. Chemistry and Properties of Nanocrystals of Different Shape. *Chem. Rev.* **2005**, *105*, 1025−1102.
(11) Bodnarchuk, M. I.; Kovalenko, M. V.; Heiss, W.; Talapin, D. V. Energetic and Entropic Contributions to Self-Assembly of Binary Nanocrystal Superlattices: Temperature as the Structure-Directing Factor. *J. Am. Chem. Soc.* **2010**, *132*, 11967−11977.
(12) Murray, C. B.; Kagan, C. R.; Bawendi, M. G. Self-Organization of CdSe Nanocrystallites into Three-Dimensional Quantum Dot Superlattices. *Science* **1995**, *270*, 1335−1338.
(13) Zaitseva, N.; Dai, Z. R.; Leon, F. R.; Krol, D. J. Optical Properties of CdSe Superlattices. *J. Am. Chem. Soc.* **2005**, *127*, 10221−10226.
(14) Kenrick, J. W.; Tisdale, W. A.; Leschkies, K. S.; Haugstad, G.; Norris, J. D.; Aydil, S. E.; Zhu, K. Y. Strong Electronic Coupling in Two-Dimensional Assemblies of Colloidal PbSe Quantum Dots. *ACS Nano* **2009**, *3*, 1532−1538.
(15) Ghosh, S. K.; Pal, T. Interparticle Coupling Effect on the Surface Plasmon Resonance of Gold Nanoparticles: From Theory to Applications. *Chem. Rev.* **2007**, *107*, 4797−4862.

(16) Zhao, W.; Ghorannevis, Z.; Chu, L.; Toh, M.; Kloc, C.; Tan, P.-H.; Eda, G. Evolution of Electronic Structure in Atomically Thin Sheets of WS2 and WSe2. *ACS Nano* **2012**, *7*, 791−797.
(17) Shi, H.; Yan, R.; Bertolazzi, S.; Brivio, J.; Gao, B.; Kis, A.; Jena, D.; Xing, H. G.; Huang, L. Exciton Dynamics in Suspended Monolayer and Few-Layer MoS2 2D Crystals. *ACS Nano* **2012**, *7*, 1072−1080.
(18) Jeong, S.; Yoo, D.; Jang, J.-T.; Kim, M.; Cheon, J. Well-Defined Colloidal 2-D Layered Transition-Metal Chalcogenide Nanocrystals via Generalized Synthetic Protocols. *J. Am. Chem. Soc.* **2012**, *134*, 18233−18236.
(19) Beal, A. R.; Knights, J. C.; Liang, W. Y. Transmission Spectra of Some Transition Metal Dichalcogenides: I. Group IVA: Octahedral Coordination. *J. Phys. C: Solid State Phys.* **1972**, *5*, 3531−3539.
(20) Auluck, S.; Reshak, A. H. Electronic and Optical Properties of the 1T Phases of $TiS_2$, $TiSe_2$, and $TiTe_2$. *Phys. Rev. B* **2003**, *68*, 245113−245120.
(21) Yun, W. S.; Han, S. W.; Hong, S. C.; Kim, I. G.; Lee, J. D. Thickness and Strain Effects on Electronic Structures of Transition Metal Dichalcogenides: 2H-$MX_2$ Semiconductors (M=Mo, W; X=S, Se, Te). *Phys. Rev. B* **2012**, *85*, 033305.
(22) Lim, S. J.; Kim, W.; Shin, S. K. Surface-Dependent, Ligand-Mediated Photochemical Etching of CdSe Nanoplatelets. *J. Am. Chem. Soc.* **2012**, *134*, 7576−7579.
(23) Thomson, J. W.; Cademartiri, L.; MacDonald, M.; Petrov, S.; Calestani, G.; Zhang, P.; Ozin, G. A. Ultrathin $Bi_2S_3$ Nanowires: Surface and Core Structure at the Cluster-Nanocrystal Transition. *J. Am. Chem. Soc.* **2010**, *132*, 9058−9068.
(24) Han, J. H.; Lee, S.; Yoo, D.; Lee, J. H.; Jeong, S.; Kim, J.-G.; Cheon, J. Unveiling Chemical Reactivity and Structural Transformation of Two-Dimensional Layered Nanocrystals. *J. Chem. Soc. Rev.* **2013**, *135*, 3736−3739.
(25) Park, K. H.; Choi, J.; Oh, D. H.; Ahn, J. R.; Son, S. U. Unstable Single-Layered Colloidal $TiS_2$ Nanodisks. *Small* **2008**, *7*, 945−950.
(26) Unpublished results.